

Photothermal/microwave radiometry for imaging and temperature feedback

Vladimir P. Zharov^a, Sergey G. Vesnin^b, James Y. Suen^c, Steven E. Harms^d

^aPhilips Classic Laser Biomedical Laboratory, ^cDepartment of Otolaryngology, ^dDepartment of Radiology, University of Arkansas for Medical Sciences, Little Rock, AR, 72205;

^bRES, Ltd., Moscow, Russia, 107082

ABSTRACT

The goal of this work is to analyze the capabilities of a new photothermal (PT) radiometry system to control temperature during laser thermal therapy. The main feature of this system is the combination of two spectral channels: infrared (IR) and microwave (MW) ranges. The first channel provides information about the temperature distribution around the surface and subsurface of absorbing structures. The second channel provides information about the localized laser-induced thermal effects occurring much more deeply, up to 3-5 cm. Experimental *in vitro* data obtained with a near-IR diode laser are presented, focusing on the estimated capabilities of the new MW radiometry as a system for providing feedback control for interstitial laser therapy. Further modifications of this system are suggested for PT radiometric confocal microscopy. The modifications are based on the combination of PT radiometry in time-resolved and frequency-domain modes, with confocal microscopy using reflected scanning modes. The potential advantages of these new approaches are discussed, including the imaging of tissue chromophores with high spatial resolution based on radiometric measurements of laser-induced thermal gradients.

Key words: Lasers, photothermal radiometry, microwave, interstitial laser therapy, feedback

1. INTRODUCTION

Photothermal radiometry (PTR) is a known technique based on the detection of increased black-body radiation from a laser-heated sample.¹⁻⁴ In the life sciences, PTR applications have included examination of optical and thermal skin properties,⁵⁻⁷ feedback control during laser thermal therapy,⁸⁻⁹ etc. (see review in Vitkin et al.¹⁰). Because of strong absorption of IR radiation, PTR *in vivo* measurements are limited to tissues that can be directly viewed by IR detectors through a lens-based optical system (skin, teeth, etc.). To measure IR radiation from deeper zones, IR fibers can be used,¹¹ but this approach still has some limitation due to the absence of non-toxic small-diameter IR fibers available for medical application. Recently, we suggested an alternative approach based on detection of microwave (MW) radiation from the laser-heated zone.¹² The advantage of this approach is relatively good transparency of biological tissues for MW radiation, which, in particular, allows using this technique in passive mode (without irradiation) for functional cancer diagnostics with a focus on breast cancer.¹³⁻²⁵ The goal of this work is to analyze the capabilities of PTR in active mode with two spectral channels, including MW range, for temperature control in subsurface zones during laser thermal treatment, as well as interstitial laser fiber-based treatment of deep zones.

2. PHOTOTHERMAL RADIOMETRY

2.1 Spectral PTR range

In accordance with Planck's law, a body at temperature T emits natural electromagnetic radiation of thermal origin with a broad spectrum from visible to radiowave and a maximum brightness B(ν ,T) at temperature 36.6°C in the mid-IR range of ~10 μ m (Fig. 1, top):^{17,25}

$$B(\nu, T) = 2h\nu^3/c^2 \{ \exp[-(h\nu/kT)] - 1 \}^{-1}, \quad (1)$$

where h is Planck's constant, ν is frequency, k is Boltzmann's constant, T is temperature, and c is the speed of light. In PTR, signal S is measured by integrating Planck's law (1) over the spectral range of the receiver ν_1 – ν_2 (or wavelength λ_1 – λ_2) and over the volume V of the heated zones, with account taken of the attenuation of IR radiation through absorption during propagation radiation from the heated zone to the receiver. In many cases, especially in IR thermography, IR emissions with the maximum power level, available in the 3–15- μm band (area I in Fig.1, top), are recorded. IR detection, however, has many drawbacks, perhaps the most serious being the small depth (micrometer range) of penetration of IR radiation in tissue: $L_{\text{IR}} = 1/\alpha_{\text{IR}}$ (α_{IR} is coefficient of absorption). For example, for most biological tissues, L_{IR} is ~ 3 – $4 \mu\text{m}$ at $\lambda_1 \sim 3 \mu\text{m}$ due to strong water absorption. Then with an increase in wavelength of just several micrometers up to 5–7 μm , depth is increased one order of magnitude, i.e., up to 30–40 μm and even to 100 μm in the mid-IR region. In tissue with little water, depth may be a little larger. Nevertheless, this spectral range allows PTR study of only surface and subsurface structures.²⁶ Information on a deeper-lying temperature distribution is only available by means of the referral of heat to the skin surface by conduction or transport mechanisms involving blood flow. In contrast, other spectral ranges in both directions from the mid-R point have much greater depth. For example, in the near-IR spectral range (0.7–1.1 μm ; area II in Fig. 1), depth is increased up to 5–9 mm, while in the MW range (3–35 cm; area III in Fig. 1) depth reaches the maximum for biological tissue—up to 3–15 cm—depending on tissue type and water amount. In both these ranges, however, the power is much lower than the mid-IR range by a factor of $\sim 10^8$. Fortunately, highly sensitive receivers are available in both ranges. In near IR, the receiver is photomultiplier cooled, and in MW range, it is a highly sensitive MW antenna. In addition, in the near IR up to 2–3 μm , it is quite possible to use nontoxic fiberoptics made from quartz with very good transparency. These circumstances allow the development of a radiometric spectral technique for evaluating the optical, thermal, and geometric properties of absorbing targets located in deep tissue.

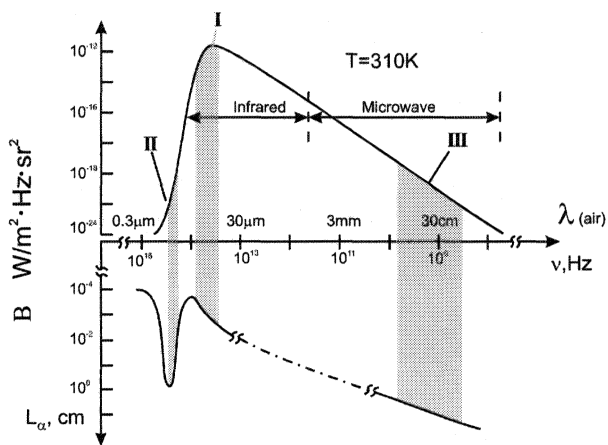


Fig. 1. Spectrum brightness for a black body (top) and depth penetration (bottom) versus frequency.

2.2 Microwave thermometry

2.2.1 Historical background

Microwave thermometry (MWR) was developed in the 1940s as a technique for sensing thermal emission, with applications in radio astronomy and remote sensing of the earth and its atmosphere. Its application in medicine was first proposed in early 1970s (see reviews in Gautherie¹⁷ and Ryan²⁵) when a contacting waveguide antenna was employed to couple MW radiation emitted by tissue into a comparison or "Dicke" radiometer working at a central frequency of 3.3 GHz. In the same period, a millimeter-wavelength scanning system employing a remote dish antenna was used to study images of superficial thermal distributions. Originally, the primary application envisaged was in screening for breast cancer. Then this technique was applied to a wide range of pathologies with associated elevated temperature, such as joint inflammation or rejection of a kidney transplant. More recently, the technique has been investigated for monitoring hyperthermia treatments. Very promising initial results have been obtained with dual-frequency (see Gautherie¹⁷) and multifrequency (five bands)²⁰ radiometry techniques capable of discriminating the temperature profile to a maximum tissue depth of ~ 4.5 cm. Others are looking at a computed MW tomography approach using a closely spaced array of MW antennas, where each antenna is pulsed one at a time in sequence around the array while recording received energy at all other antenna positions.²¹ Change et al.²² described an active imaging system with a 14.75-cm-diameter array of 16 antennas operating over the 300–900 MHz band and producing a maximum temperature precision of 0.98°C and a relative accuracy of 0.56°C . Other possible applications of MWR and its modes have been discussed by other investigators.^{15–24}

Utilizing just one antenna by changing its position, MWR also has some potential for medical applications. For example, we developed the first experimental setup with one antenna for the purpose of the functional diagnosis of breast cancer.^{12,19} The principle of MWR diagnostics was based on the detection of small temperature changes (range, 0.1– 1.8°C) due to increased cancer-cell metabolism.²⁷ In particular, clinical trials involving more than 1,000 patients at

four oncology centers in Moscow showed that the sensitivity of MT for functional breast cancer diagnosis is 89%, specificity is 78%, and accuracy 83%.^{12,19} These results are comparable with those for mammography. These data showed that MT methods allow the distinction of mastopathy and fibroadenoma with proliferation from mastopathy and fibroadenoma without proliferation. Therefore, this technique can be used to select risk-group patients. Other diagnostic techniques (X-ray, MRI, etc.) cannot do this because they detect disease on the basis of anatomic changes. Recently, we suggested using this technique to control interstitial laser therapy (ILT).¹²

2.2.2 Temperature resolution

It is known that in the MW region where $v \ll kT/h$, Planck's expression for power emitted from a black body can be approximated by the Rayleigh-Jeans expression:¹⁷

$$P = 2kT v^2/c^2, \quad (2)$$

that is, in the MW region, the power emitted by a black body is proportional to its physical temperature T . Hence, the interpretation of external measurements in terms of internal temperature distribution and calibration procedure is potentially easy, compared with that in the IR range, where at recording integrated radiation in relatively broad-spectrum signal is proportional to T^4 according to Stephan-Boltzmann's law.

The internal temperature is measured by contacting a patient's skin with the antenna at the point of the organ under investigation or of its part projection. Noise signal power at MW frequencies received by the antenna in the first approximation is calculated as¹⁷

$$P = \epsilon k T \Delta f, \quad (3)$$

where ϵ is emissivity, and Δf frequency bandwidth. When the frequency band Δf is 100 MHz, the tissue temperature is $T = 310K$, and when $\epsilon = 1$, this power is 4×10^{-13} W. According to Gautherie,¹⁷ the temperature resolution depends on the system noise temperature, the temperature of the body, the bandwidth of the radiometer, the receiver, and the integration time constants. For optimal MWR parameters at room temperature and the above mentioned parameters, temperature resolution of $0.1^\circ C$ is achievable with a time constant of 1 s.

2.2.3 Spatial resolution

Spatial resolution (lateral) is a function of both the frequency of operation and the type and size of antenna employed.¹⁷ Theoretically, the minimum spatial resolution of a contacting antenna is of the order of $\delta_{\min} = \lambda_m/2$, where λ_m is the wavelength in the medium with which the antenna is in contact: $\lambda_m = \lambda/(\epsilon)^{1/2}$, where λ is the wavelength in a vacuum and ϵ is the dielectric constant of the medium. If the antenna dimensions (diameter) are large compared with λ_m , the spatial resolution is of the order of the size of the antenna. That is why, to achieve the highest resolution, antenna size must be compared with $\lambda_m/2$ or a little smaller. For example, for the typical parameters of ϵ ¹⁷ (water, 81; muscles and skin, 50-60; brain, 30; and bone, 5-6), the theoretical minimum spatial resolution δ_{\min} for $\lambda = 26$ cm would be approximately 1.4 cm, 1.7 cm, 2.5 cm, and 5 cm, respectively. The antenna size can be reduced by propagating the electromagnetic wave in a higher dielectric constant medium within the antenna. For example, an open-ended waveguide antenna can be filled with low-loss dielectric materials with a permittivity >1 . In practice, the spatial resolution of an antenna varies in a complex manner with aperture size.¹⁷ Thus, it is possible to make some improvements in resolution in the near field by designing an antenna with a proper aperture. Our theoretical estimation shows that with the design of proper antenna parameters (aperture, geometry, dielectric loss, etc.) and with the choice of a shorter wavelength (~ 3 -10 cm) and corresponding algorithm of MWR signal treatment, it is quite possible to achieve MWR spatial resolution of the order of 0.5 cm. It is necessary to take into account that with increasing frequency MW depth penetration has a tendency to diminish.

2.2.4 Depth of penetration

Although the penetration depth is many times greater in the MW than in the IR range, this factor can still limit the application of MWR to temperature monitoring. The penetration depth depends on the frequency of operation, the tissue type, and the antenna type and size.¹⁷ Above and here, this parameter L is defined as the depth to which a signal can travel in tissue before it is attenuated by factor $1/e$. The majority of radiometry receivers operate with a central

frequency in the range of 1-5 GHz, where penetration depth is 2-4 cm in muscle and 6-15 cm in fat.¹⁷ It is interesting to note that, with a relatively strong attenuation medium, MWs traveling from the heated zone along the antenna axis, compared to waves traveling outside the axis, are attenuated less because the smaller optical path leads to a narrowing of the field of view (i.e., equivalent to some improvement of spatial resolution).

3. TEMPERATURE CONTROL DURING LASER THERMAL THERAPY

In current laser surgery, the problem of temperature control is significant, especially with the treatment of internal zones with ILT. ILT is a surgical procedure in which an optical fiber is inserted into tissue, and absorbed laser light heats and destroys the tissue near the fiber's tip by photocoagulation. Many clinical and basic studies have shown that ILT could be a very promising modality for local cancer treatment, including breast, liver, prostate, and head and neck tumors (e.g., see Muller and Roggan²⁸ and Harms et al.^{29,30}).

In ILT, both accurate temperature and time exposure determine the effectiveness of photocoagulation and therefore the final treatment outcome. It is believed that moderate heating of a tumor with a laser source to ~60-70°C produces cancer-cell necrosis through protein coagulation.²⁸ The maximum tissue temperature near the fiber tip must remain <100°C to avoid vaporization, charring, and smoke production, which potentially lead to complications such as burning, infection, inflammation, and tumor spread through water vaporization with consequent cancer recurrence. It should be noted that this temperature range differs somewhat from hyperthermic cancer therapy, in which the highest temperature is 42-43°C.

Ideally, the temperature increase produced by ILT in the treatment site must be controlled to avoid thermal damage to healthy tissue surrounding the tumor and yet to ensure total tumor-cell necrosis within the desired tissue volume without vaporization or charring. In practice, Nd:YAG and diode lasers have frequently been used for ILT. They afford deep tissue penetration of near-IR radiation, but for certain powers and exposure durations, increasing optical energy penetration may actually decrease the coagulation lesion volume. Thus, a high-power, short-time-exposure, precharring mode is utilized, as it consistently permits an increased temperature in the necrosis zone. Due to nonuniform temperature distribution and charring, however, this method may cause the previously noted complications. This effect is more significant for plane-cut fiber ends. More promising alternatives are optical spherical, cylindrical diffusers or different modifications of metal tips, but the high concentration of absorbed energy around them and the relatively longer time needed to heat a large tumor from the local metal tips remain other problems.

Therefore, in most existing treatment methods (e.g., Harms et al.^{29,30}), only the precharring mode with short-term heating >100°C was used, mainly to increase absorption and heating around the fiber. This means that the main potential advantages of laser treatment due to better volume coagulation were not quite realized. If precharring mode is used, the laser heats only the small, carbonized area around the fiber, and this area works like thermal point source. This can be realized more easily with electrical heating or laser heating of the metal tip at the fiber's end.

The *in situ* interstitial temperatures generated during clinical or experimental laser irradiation are generally measured with different techniques, including thermocouple probes, IR thermometry with IR fibers, optical temperature sensors such as temperature-sensitive fluorescent probes, ultrasonography, and MRI.^{17,25} All of these techniques, however, are not available for continuous temperature monitoring during ILT, or they are limited by poor accuracy, inconvenience in interstitial application, small spatial area of monitoring, and so on. For example, PTR requires the use of an IR fiber, which has some limitations, including toxicity of the IR fiber material and the increased fiber size needed to provide good sensitivity. Recently, MRI was successfully used to monitor temperature during ILT,³¹ but it is still a very complex, expensive technique that does not allow the measurement of temperature around a metal MRI-compatible needle. Thus, the principal limitation of current MRI technology is that the metal needle used to place and fix the fiber's position during ILT obscures the information needed for thermal measurement. Fibers with special coatings for MRI visualization are still in the experimental stage.

Thus, in general, ILT is a promising modality for breast cancer treatment, although it still has some limitations. These include no intraoperative real-time temperature dosimetry of laser-induced thermal effect; poor understanding of the optimal temperature range; relatively high temperature gradient at the tip of the optical fiber; a nonuniform thermal lesion; potential complications after overheating and charring, such as burning, infection, and inflammation; tumor spread through water vaporization; and residual disease from inadequate ILT. Laser parameters were usually chosen on the basis of common recommendations from practice.

4. PTR/MWR IN LASER THERAPY AND DIAGNOSIS

Methods and schemes used in MWR/PTR depend on the medical tasks. There are two main tasks: (a) temperature control during laser treatment and (b) investigation of a tissue's optical and thermal properties.

4.1 Temperature control

Laser treatments have two main spatial geometries: (a) surface treatment and (b) interstitial treatment using a fiber to deliver laser radiation into a tissue (Fig. 2).

In the first scheme, a laser illuminates the surface, and volume treatment depends on the penetration depth of laser radiation into tissue (L_L). Laser-induced heat absorbed through surface and subsurface targets (cell chromophores, skin melanin, blood in vessels, hair follicles, etc.) depends on laser power and the medium's coefficient of absorption, and may vary from 42-43°C (laser hyperthermia) to 60-70°C (coagulation) and >100°C (ablation, vaporization, and carbonization, etc.) according to the medical task. Heating of absorbing targets causes increased black-body radiation detected by IR or MW arrays. Signals depend on the relations among the depth of laser penetration (L_L), the depth of IR penetration (L_{IR}), the depth of MW penetration (L_{MW}), and the depth of the absorbing targets (L_T). Two cases important for practice:

1. Surface treatment: $L_L \sim L_T$; $L_L \ll L_{MW}$; and $L_T < L_{IR}$. In this case, MWR does not play a significant role because PTR in the IR range can control surface temperature. MWR, however, can help obtain additional information for estimating subsurface temperature distribution at depths of 100-500 μm and greater if PTR in the IR range does not already work because of strong absorption of IR radiation.
2. Volume treatment: $L_L \sim L_T$; $L_T \gg L_{IR}$; and $L_T < L_{MW}$. This is the optimal application of MWR while PTR in the IR range is used as a reference channel to control surface temperature in order to increase the accuracy of MWR measurements.

In the ILT scheme, depth of penetration of the fiber end L_F meets the condition $L_F \gg L_{IR}$, and in the case of $L_{MW} > L_F$ the MWR system usually allows control of the average volume temperature around the fiber end.

4.2 Tissue diagnostics

Compared with its use in the previous case, laser is used just to probe tissue by heating at low temperature (no more than 1-5°C) without thermal destruction. This technique is used to measure chromophore distribution in tissue and the coefficient of absorption or to estimate thermal properties. There are two main PTR modes: (a) time-resolved PTR with pulsed laser^{5,10} and (b) frequency-domain PTR with continuous modulated laser.³² In the first mode, the pulsed radiometric signal is the sum of signals from different depths of the irradiated volume. So analysis of the time-shape signal yields some information about temperature and chromophore distribution, respectively, in the subsurface structure. In the second mode, amplitude and phase of the radiometric signal depend on the optical and thermal properties of the tissue, which allow the use of this technique for profilometric imaging of tissue. In many experiments, however, lateral spatial resolution was not studied in detail. High lateral resolution in PTR can be achieved by two ways: (a) tight focusing (up to 1 μm) of the excitation beam and the use of a spatially confined IR system for detecting IR radiation from small laser-heated area and (b) using a broad laser excitation beam and a high-resolution IR system for detecting IR radiation from different zones

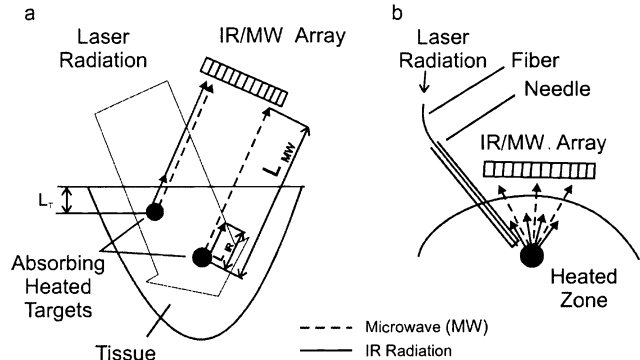


Fig. 2. MWR/PTR monitoring of temperature during surface laser treatment (a) and ILT (b).

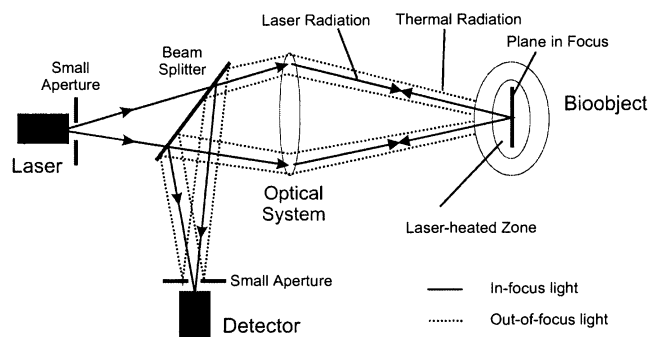


Fig. 3. Schematic of confocal photothermal microscopy in the near-IR range.

of heated volume. It is possible to have quite different combinations of these approaches.

To achieve high resolution, we recently suggested a new scheme-confocal PTR (CPTR)-based on the combination of PTR with conventional confocal microscopy.³³ It is known that a conventional confocal microscope differs from a standard light microscope in its use of a point sources of light, typically a laser, to illuminate a small spot that can be scanned with tissue (Fig. 3). With spatial filtering of reflected laser light through a pinhole, an image is created from a thin "plane of interest" that is in focus. Out-of-focus light returning from tissue that is superficial or deep to the focal plane is rejected. With this device, thin "optical sections" of biological specimens can be imaged at a resolution similar to that of light microscopy. In conventional confocal microscopy, image contrast is determined by the natural differences in refractive indices (light-scattering properties) or fluorescence of subcellular structures within tissues. Operating parameters of modern confocal reflectance microscopy usually include diode laser illumination (e.g., wavelength of 830 nm, 30× objective lens, 0.9 NA, water immersion), and the maximum depth of imaging is 400 μm. Such a system provides a lateral resolution of 1 μm and a virtual tissue "section" thickness (axial resolution) of 5 μm when unstained tissue is imaged. In the new CPTR, laser is used to heat absorbing targets from which IR radiation is detected with a highly sensitive near-IR detector (cooled photomultiplier with a spectral range of 0.7-95 μm and JnSb in the spectral range of 1.5-5 μm) with a diaphragm in front of its face. In the near-IR range (0.7-3 μm), it is quite possible to use a conventional-scheme confocal microscope with a lens system (Fig. 3).

In the mid-IR spectral range (5-15 μm), it is more convenient to use a mirror system and a relatively high-sensitivity liquid nitrogen-cooled HgCaTe as an IR detector (Fig. 4). Imaging is produced by scanning the sample. Instead of a single IR detector, an array of IR detectors can be used. Because of the relatively small amount of IR radiation, scheme must have maximum sensitivity. The IR emission from the sample must be monitored with the above mentioned high-sensitivity cooled IR detectors and lock-in amplifier. Detectors are placed in the focal plane of the IR (germanium) lens or mirror. Lateral resolution will depend on the laser spot size and the pinhole size in front of the IR detectors.

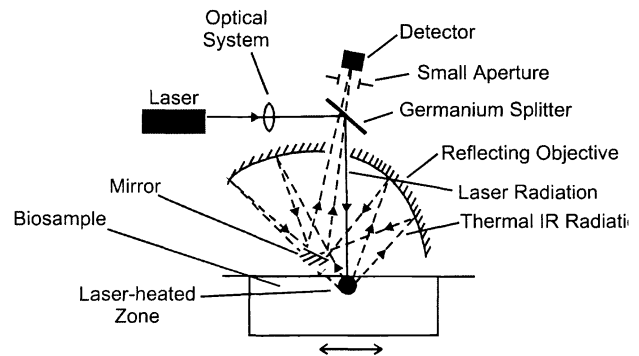


Fig. 4. Schematic of confocal photothermal microscopy in the mid-IR range.

5. RESULTS

The main goal of this experimental research was to test the described hypotheses and approaches. In this section, we present experimental data only on the capability of the MW system. Despite the long history of the MW technique, there is an evident lack of estimates of its sensitivity and spatial resolution when applied to controlling hypothermia and laser thermal treatment. That is why the objective of our preliminary work was to estimate the capability of MWR in monitoring temperature effects during ILT. Moreover, because MWR is a relatively new diagnostic modality in laser therapy, it requires the development of a corresponding new metrologic basis.

The underlying hypothesis of these experiments was that MWR can noninvasively and remotely control thermal effects during local ILT. This hypothesis has been verified experimentally *in vitro* on some biotissue samples (chicken breast, porcine tissue, etc., which were cut into square sections with maximum dimensions of 3×4×3 cm). The experimental setup is shown in Fig. 5.

Laser radiation is delivered to the samples through a quartz optical fiber with core diameter 600 μm. A continuous-wave diode laser (Diomed, Cambridge, UK) operating at wavelength 805 nm with output power in the

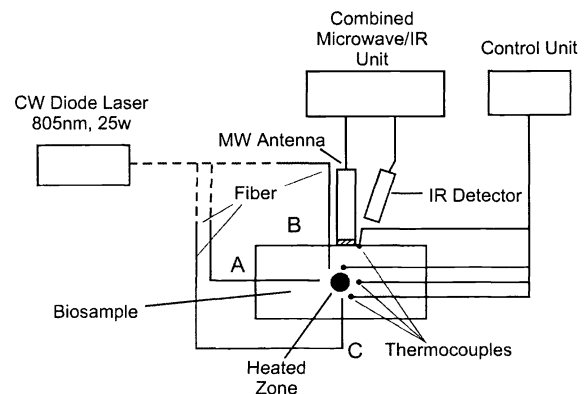


Fig. 5. Experimental setup.

range of 0.5-25 W and exposure times from 1 to 10 min was used as an optical source for ILT. The fiber end can be inserted into the tissue sample with medical 18-gauge hollow needle at different depths and directions: through sample side parallel of the surface (A), through the top surface (B), and through the bottom surface (C).

The MW antenna is built as a printed cylindrical vibrator with a 39-mm diameter and a frequency of ~ 1.15 GHz. To measure small differences in temperature on the order of 0.2°C (power difference on the order of 10^{-15} W), we used the so-called modulated null-radiometer with a slipping circuit scheme to compensate for reflective effects on the skin surface. The feature of this scheme is a periodical comparison of external temperature with internal temperature generated by the electrically heated resistor. To increase accuracy and control surface temperature to prevent burning effects around the needle entrance in the skin, we used in addition a sensitive pyroelectric IR detector with a lock-in amplifier built into the MW device to realize a PTR method with a spectral range of 5-15 μm . It was necessary for additional laser dosimetry during ILP. Independently, a thermocouple array controlled temperature at different distances from the fiber end.

We experimentally evaluated MWR's spatial resolution and sensitivity by scanning the MW antenna across the sample or by changing the position of the fiber in the tissue when the small laser-heated area around the fiber end played the role of a point thermal source. Thus, the MW antenna, thermocouples, and IR detector independently monitored the internal and surface temperatures of the sample in the range of 18-80°C. The MW antenna (radiometric probe) was in contact with the biotissue to achieve good impedance matching. An IR detector in the mid-IR range was used for PT control of surface temperature in two zones: (1) close to the fiber end and (2) around the needle entrance into the issue; this range provides more reliable protection against possible burning of the skin surface due to diffusion of heat from the laser-heated zone.

Before application, the MWR system was calibrated by absolute temperature. For the calibration, the MW antenna, insulated by a Mylar sheet, was placed on a thermostated water bath (YSI 4600 Precision Thermometer; YSI Inc., Yellow Springs, OH) whose temperature was raised at 1°C intervals from 25°C to 80°C . Results of water temperature measurements with the built-in thermostat thermometer (horizontal axis), MW antenna, and electric thermometer are shown on Fig. 6.

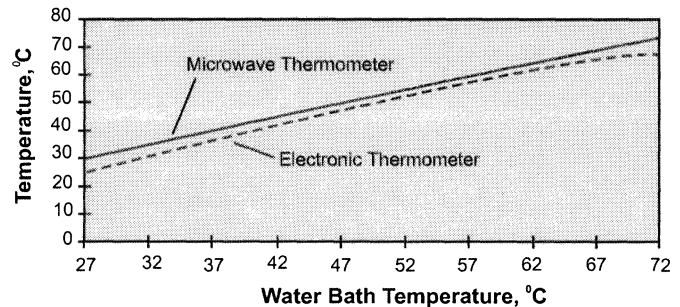


Fig. 6. Calibration of the MW antenna with a water thermostat.

Both modalities showed approximately the same results, and both curves were linear, except at relatively high temperatures $>60^\circ\text{C}$. The difference in absolute temperature obtained with MW and electronic thermometry was introduced especially to see the character of both curves more clearly. The average MWR accuracy in the $27\text{-}37^\circ\text{C}$ range was $\sim 0.2^\circ\text{C}$. Its accuracy in ranges higher than 37°C was poorer, $\sim 0.5\text{-}1.2^\circ\text{C}$. It should be noted that initially the MW antenna was developed for use in cancer diagnostics at exactly the $27\text{-}37^\circ\text{C}$ range.

Preliminary estimation of the capability of the combined experimental setup was carried out during laser irradiation of the porcine surface *in vitro*. The fiber end was inserted only 2 mm into the tissue surface, and surface temperature was measured by thermocouples placed on the surface close to the fiber and the IR detector recording IR radiation around the fiber from the surface (Fig. 7).

With increased power, the temperature rises, and at higher powers, the fast, dramatic temperature rise is associated with charring effects at the fiber end. The same results were obtained

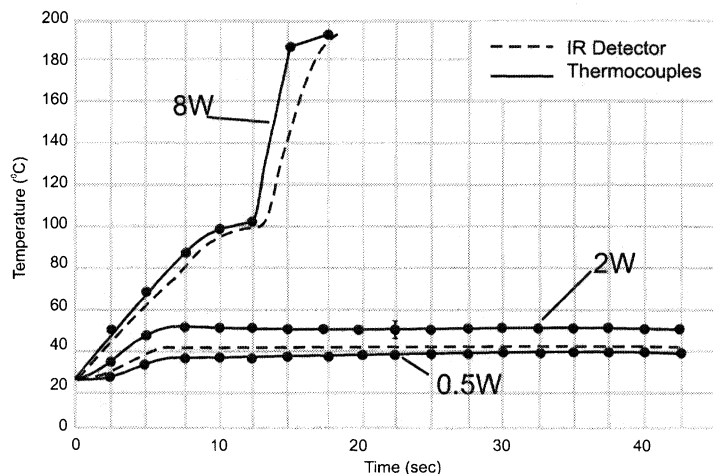


Fig. 7. Porcine surface temperature during irradiation with an 805-nm laser at different powers on distance 2 mm from the fiber end (along surface).

with an IR detector with a Ge filter to block the direct effect of laser radiation. It is interesting to note that fast-heating effects ($>100^{\circ}\text{C}$) took place several times at relatively lower powers (4-6 W), which can be explained by noncontrolled charring in hot spots or the presence a small, strongly absorbing particle in the tissue. It is necessary to note that at calibration with controlled heating of the smooth black surface, the absolute accuracy of the IR detector was high ($\sim 0.2^{\circ}\text{C}$). A relatively lower accuracy obtained in these experiments can be explained by the nonsmooth local distribution of heat around the fiber.

The experiments using fiber only and fiber guided by a metal needle showed the same results, i.e., that the presence of a metal needle does not significantly affect the MW antenna. Injection of a 1% indocyanine green (ICG) solution in the area around the fiber end allowed a ~ 5 -6-fold increased signal from the MW antenna.

Fig. 8 shows the results of temperature measurement in chicken breast at different laser powers when fiber end was placed in position A (Fig. 4) in the center of the MW antenna at 1 cm from the surface. It is clear that the MW antenna signal depends on time expose and laser power.

Some fluctuation in signal can be explained by the influence of a relatively strong electromagnetic noise emitted from a nearby mechanical room. Signal was much more stable in the absence of electromagnetic noise or with the use of a metallic shield around the MW antenna. In this type of experiment, however, we used only a naked MW antenna and did not attempt to reduce noise. Nonetheless, the data we obtained clearly demonstrated the circumstances in which the MW antenna can be used to monitor ILT. On the vertical axis only arbitrary units were used because careful temperature calibration of absolute measurements is needed, especially as MW signal also depends on the geometry and shape of the heated zone. In our experiments with thermocouple control, we found that the size of the heated zone around the fiber end was 6-8 mm in diameter and this zone had in first approximation a gaussian temperature distribution along the radius.

Fig. 9 shows the signal dependence from the MW antenna on the position of the fiber end across the tissue at the same laser power and exposure time (3W, 10 min) at two discrete distances (1 cm and 2 cm) from the tissue surface. These data demonstrate the spatial resolution of the MW antenna is equal to 2.2 cm for a 1-cm depth and 1.8 cm for a 2-cm depth. This is very close to theoretical resolution, although we do not know the exact water content and proportions of fat and muscle in the chicken breast. A little better resolution for deeper targets can be explained by the relatively large diameter of the MW antenna used and the slight differences in MW paths from the local heated zone to the different surfaces of the MW antenna.

Fig. 10. shows MW signal dependence on the distance between the fiber end and the surface for two spatial geometries of fiber insertion into tissues (Fig. 4, positions C and B). The sensitivity of the MW antenna allows the measurement of

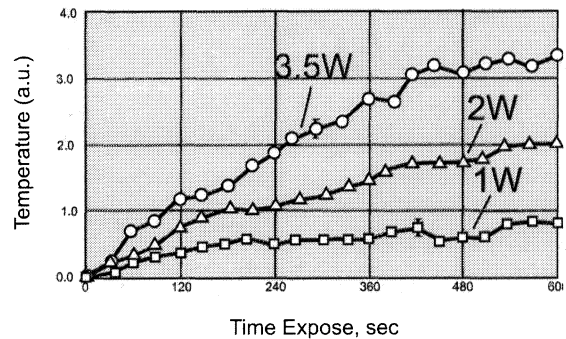


Fig. 8. MW antenna signal as a function of laser power and exposure time with the fiber located 1 cm from the chicken breast surface.

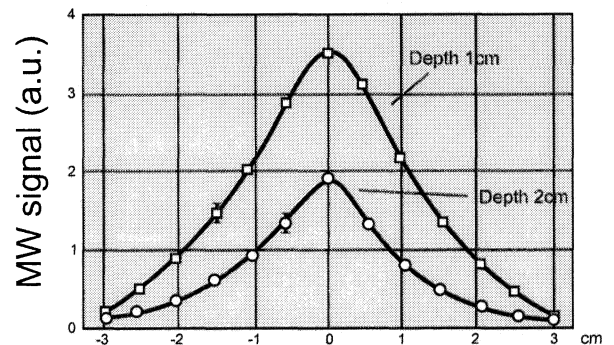


Fig. 9. MW signal as function position the fiber end across sample at two different distance from surface (1 cm and 2 cm).

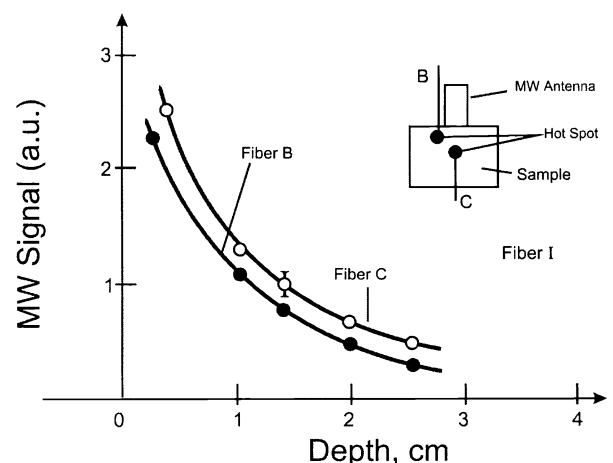


Fig. 10. MW signal as a function of the depths of point thermal sources for two spatial fiber positions.

temperatures to a depth of at least 2.5 cm for such an inconvenient object as chicken breast with high water and muscle content. In the case of position C the thermal source is closer to the surface than the fiber end and on contrary in case B a little far respectively. We had an available sample with a depth of ~3 cm, and we could not check sensitivity at the deeper zone. At a depth of 2.6 cm, however, we had sufficient signal-to-noise ratio that extrapolation to level noise yielded an estimate of the maximum depth of temperature detection as 4 cm at a laser power of 2 W and a time exposure of 10 min. For tissue containing less water, we can estimate to depths of ~6-7 cm.

6. CONCLUSION

Thus, we have developed a combined MWR/PTR system with the following characteristics: maximum depth of detection of a laser-heated zone: 4-6 cm (depending on the water content and type of tissue); cross-sectional spatial resolution: 1.8 cm (half width 50% level); measuring time: 3-5 sec; sensitivity threshold of average relative deep temperature variation: 0.2°C; accuracy of measuring the skin temperature: 0.2°C.

Absolute temperature accuracy at different temperature ranges was 0.5-1.2°C, with the assumption that the temperature profile around the fiber was smooth. It should be noted that to prevent tissue charring, it is necessary to maintain the temperature and corresponding laser power just below some critical level (e.g., <90-100°C). This is why the requirements for accurate MW feedback could not be so strict, but a statement of this kind needs additional study. Our hope, however, is that in the future with knowledge of the spatial location of a tumor from MRI, the average typical size of the heated zone, and additional experimental data, we will develop an algorithm that can be used to keep temperature in a tighter range of at least 60-70°C, or perhaps even tighter, with the MW antenna. This system could also be very useful for studying subsurface chromophore profiles in tissues at different depths of laser penetration in combination with PTR. Another critical question concerns the spatial resolution requirements. For example, on the one hand, high resolution is useful for estimating temperature distribution, but on the other hand the MW signal in this case will be sensitive to the spatial position of the MW antenna; thus additional effort will need to be directed to stabilizing the antenna position. This question also needs further theoretical and experimental study to find a compromise.

This technique also holds promise for guiding the laser treatment of other types of diseases, including prostate cancer and the phototreatment of lymphedema after mastectomy. Its parameters can be further improved to provide depth measurements up to 8 cm and a sensitivity of 0.1°C, as well as the use of a multifrequency, multichannel MW array to obtain 3-D images of the heated zone with a resolution of 0.5-1 cm. Such improvements are quite sufficient for the treatment of tumors >3-4 cm. During scanning with a focused laser beam, this technique allows obtaining images with high optical resolution, depending on the laser spot. With some modification, this technique can be used to control heat induced by other types of energy, including focused ultrasound and electromagnetic waves.

ACKNOWLEDGMENTS

The authors are grateful to Scott Scrape, who assisted at preliminary stage of experiments with the MW system, and to Scott Ferguson (Philips Classic Laser Biomedical Laboratory, University of Arkansas for Medical Sciences) for assistance with calibration of the MW system. We also thank the UAMS Office of Grants and Scientific Publications for editorial assistance during the preparation of this manuscript. This work was supported by funding from the Arkansas Breast Cancer Research Program and the Medical Research Endowment fund of the University of Arkansas for Medical Sciences.

REFERENCES

1. P.E. Nordal and S.O. Kanstad, "Visible-light spectroscopy by photothermal radiometry using an incoherent source," *Appl. Phys. Lett.*, **38**, pp. 486-488, 1981.
2. A.N. Zhitov, V.P. Zharov, A.V. Kuznetsov, et al., "IR radiometry with CO₂ laser for remote control of absorbing targets," Proceedings of the all-union symposium on technical tool of control of environments. Leningrad, 1981, paper # 98.
3. W.P. Leung and A.C. Tam, "Technique of flash radiometry," *J. of Appl. Phys.* **56**, pp. 156-161, 1984.
4. R.E. Imhof, D.J.S. Birch, F.R. Thornley, et al., "Optothermal transient emission radiometry," *J. of Phys. E: Sci. Instrum.* **17**, pp. 521-525, 1984.

5. G.P Chebotareva, A.M Prokhorov, V.P Zharov, et al. "Optical and thermal properties of tissue studied by pulsed photothermal radiometry," *Preprint of Academy of Sciences of the USSR, Institute of General Physics, #146, Moscow, 1987.*
6. F.H Long, R.R Anderson, and T.F. Deutsch. "Pulsed photothermal radiometry for depth profiling of layered media," *Appl. Phys. Lett.* **51**, pp. 2076-2078, 1987.
7. A.M Prokhorov, G.P Chebotareva, V.P. Zharov, et al., "Pulsed photothermal radiometry of bio-objects with CO₂, Nd:YAG and Er:YAG lasers," *J. of Quantum Electron.* **46**, pp. 1981-1996, 1989.
8. V.P Zharov and A.A Kozlov, "Optocalorimetric methods for registration of phase transition in laser irradiated biomedical medium," Proceedings of the VIth international topical meeting on photoacoustic and photothermal phenomena, Baltimore, July 31-August 3, pp. 114-116, 1989.
9. V.P Zharov, "Principle of photothermal control in laser surgery," Proceedings of the VIIth international meeting on photoacoustic and photothermal phenomena, the Netherlands, pp. 84-86, 1991.
10. Vitkin, B.C Vilson, and R.R Anderson, "Pulsed photothermal radiometry studies in tissue optics," in: A.J. Welch, et al. (eds.), *Optical-Thermal Response of Laser-irradiated Tissue*, pp. 535-560, Plenum Press, New York, 1995.
11. A. Zur and A. Katzir, "Use of infrared fiber for low temperature radiometric measurements," *Appl. Phys. Lett.* **48**, pp. 499-502, 1986.
12. V.P Zharov, S.G. Vesnin, S.E Harms, J.Y Suen, A.V. Vaisblat, and N. Tikhomirova, "Laser combined interstitial cancer therapy with microwave temperature and RODEO MRI feedback. Part 1. Microwave radiometry," *Proc. SPIE*, **4257**, pp. 370-376, 2001.
13. A. Barrett, P.C. Myers, and N.L. Sadowsky, "Detection of breast cancer by microwave radiometry," *Radio Sci.* **12** (68), pp. 167-171, 1977.
14. P.C Myers, N.L. Sadowsky, and A.H. Barrett, "Microwave thermography: principles, methods and clinical applications," *J. of Microwave Power* **14** (20), pp. 45-51, 1979.
15. Y. Leroy, "Microwave radiometry and thermography: present and prospective," in: M. Gautherie and E. Albert (eds.), *Biomedical Thermology: Proceedings of an International Symposium Held in Strasbourg, France, June 30-July 4, 1981*, pp. 485-499, Alan R. Liss, New York, 1982.
16. K.L Carr, "Microwave radiometry: its importance to the detection of cancer. *IEEE MTT*, **37** (12), pp. 19-24, 1989.
17. M. Gautherie (ed.), "Methods of hyperthermia control," Springer-Verlag, Berlin, 1990.
18. E. Godik and Y. Guliaev, "Functional imaging of the human body: dynamic mapping of physical E-M fields signals a breakthrough in medical diagnostics," *IEEE Engineering Med. Biol.* **10** (4), pp. 67-75, 1991.
19. L.M. Burdina, A.V Vaisblat, S.G Vesnin, et al., "Detection of breast cancer with microwave radiometry (in Russian)," *J. of Mammol.* **2**, pp. 2-15, 1998.
20. S. Mizushina, T. Shimizu, and T. Sugiura, "Non-invasive thermometry with multifrequency microwave radiometry," *Front. of Med. Biol. Engineering* **4**, pp. 129-133, 1992.
21. P.M Meany, et al., "Non-active antenna compensation for fixed-array microwave imaging, parts I and II," *IEEE Trans. Med. Imaging* **18**, pp. 496-519, 1999.
22. J.T. Change, et al., "Non-invasive thermal assessment of tissue phantom using an active near field microwave imaging technique," *Int. J. of Hyperthermia* **14**, pp. 513-534, 1998.
23. V.M. Polyukov, "Application of high-frequency radiometry in medicine and veterinary," *Biomed. Electronics* **2**, pp. 87-95, 1999.
24. V. L. Anzimirov, et al., "Investigation of thermal excitation in a human head brain at functional test by the method of dynamic multiprobe radiothermoimaging," *Biomed. Radioelectronics* **3**, pp. 22-30, 2000.
25. T.P. Ryan, "Matching the energy sources to the clinical need," *Proc. SPIE, Critical Reviews, CR75*, pp. 327-367, 2000.
26. W. Majaron, B. S. Verkruysse, B. Tanenbaum et al., "Pulsed photothermal profiling of hypervascular lesions; some recent advances," *Proc. SPIE* **3907**, pp. 114-125, 2000.
27. M. Gautherie, "Biomedical thermology," in: M. Gautherie and E. Albert (eds.), *Biomedical Thermology: Proceedings of an International Symposium Held in Strasbourg, France, June 30-July 4, 1981*, pp. 21-64, Alan R. Liss, New York, 1982.
28. G. Muller and A. Roggan (eds.), *Laser-induced Interstitial Thermotherapy*, SPIE Optical Engineering Press, Bellingham, Washington, 1995.

29. S.E. Harms, H. Mumtaz, V.S Klimberg, et al., "Laser lumpectomy with interactive MR imaging: histopathologic correlation," *Radiology* **209**, pp. 468-475, 1998.
30. S.E. Harms, H. Mumtaz, B. Hyslop, et al., "RODEO MRI-guided laser ablation of breast cancer," *Proc. SPIE* **3590**, pp. 484-489, 1999.
31. H. Atsumi, M. Matsumae, M. Kaneda, et al., "Novel laser system and laser irradiation method reduced the risk of carbonization during laser interstitial thermotherapy: assessed by MR temperature measurements," *Laser Surg. Med.* **29**, pp. 108-117, 2001.
32. L. Nicolaides, A. Mandelis, S.H. Abrams, "Novel dental dynamic depth profilometric imaging using simultaneous frequency-domain infrared photothermal radiometry and laser luminescence," *J. of Biomed. Opt.* **5**, pp. 31-39, 2000.
33. R.H. Webb. "Confocal optical microscopy," *Rep. Prog. Phys.* **59**, pp. 427-471, 1996.